**Discover** Oncology

Research

# 5,7,2′,6′- Tetrahydroxyflavone affects the progression of ovarian cancer via hsa-miR-495-3p-ACTB/HSP90AA1 pathway

**Mengjie Chen[1,2] · Huihui Jia[3] · Xuyang Tao[4] · Yani Jin[2] · Zuorong Shi[5]**

Received: 10 December 2024 / Accepted: 5 May 2025
Published online: 19 May 2025


## Abstract

**Background** *Scutellariae Radix* (SR), a traditional Chinese medicine, has been shown to have potential anti-cancer properties.

**Purpose** To explore the mechanism of inhibiting ovarian cancer (OC) progression by SR.

**Methods** The key active ingredient (5,7,2′,6′-Tetrahydroxyflavone, TF) and key targets (ACTB and HSP90AA1) of SR were screened by the network pharmacology method. CCK-8 reagent, Transwell assay, and Annexin-V-FITC kit were used to evaluate the effects of TF on OC cell viability, migration, and apoptosis. The upstream microRNAs (miRNAs) of ACTB and HSP90AA1 were predicted by the starBase database. Important miRNAs related to OC were mined using gene expression datasets in the GEO database. RT-qPCR and Western blotting experiments were used to detect miRNA or gene expression.

**Results** TF inhibited OC cell viability/migration and induced apoptosis in a concentration-dependent manner. Hsa-miR-495-3p was identified to be a key miRNA in OC, whose expression was lacking in OC cells. ACTB and HSP90AA1 expressed highly in OC cells. Hsa-miR-495-3p mimics reduced ACTB and HSP90AA1 expression. Hsa-miR-495-3p inhibitor and overexpression of ACTB or HSP90AA1 reversed the inhibitory effect of TF on OC cells.

**Conclusion** TF, an active ingredient of SR, hindered OC progression through the hsa-miR-495-3p-ACTB/HSP90AA1 pathway.

## Highlights

1. SR has the potential to inhibit OC progression through multi-target and multi-pathway.
2. TF was identified as an important active ingredient of SR in inhibiting OC progression.
3. TF inhibited migration and induced apoptosis of OC cells through the hsa-miR-495-3p-ACTB/HSP90AA1 pathway.

**Keywords** *Scutellariae Radix* · Ovarian cancer · Hsa-miR-495-3p · ACTB · HSP90AA1

Mengjie Chen and Huihui Jia have contributed equally to this work.

**Supplementary Information** The online version contains supplementary material available at https://doi.org/10.1007/s12672-025-02570-8.

✉ Zuorong Shi, zuorongshi963@163.com | [1]School of Chinese Medicine, Shandong University of Traditional Chinese Medicine, Jinan 250355, China. [2]Department of Gynecology, Xi 'an Hospital of Traditional Chinese Medicine, Xi 'an 710000, China. [3]Department of Gynecology and Obstetrics, Xi 'an No.1 Hospital (High-tech campus), Xi 'an 710100, China. [4]Traditional Chinese Medicine Department, Xi 'an No.1 Hospital (High-Tech Campus), Xi 'an 710100, China. [5] Admission Office, Shandong University of Traditional Chinese Medicine, No. 4655 University Road, Science and Technology Park, Changqing District, Jinan 250355, Shandong, China.

## 1 Introduction

Ovarian cancer (OC) is the deadliest gynecological cancer in the world, killing more than 152,000 people each year [1]. The 5-year survival rate for patients with OC is only 47% [2]. The drug treatment of OC is mainly chemotherapy drugs, such as paclitaxel, and some platinum drugs such as oxaliplatin, cisplatin, carboplatin, and so on [3]. However, these drugs are prone to many side effects in the process of use, such as nausea, hair loss, liver and kidney function abnormalities. Drug resistance caused by the long-term use of chemotherapy drugs is also a difficult problem in OC treatment.

Traditional Chinese medicine therapy has a long history in China with a gentler role, and there is much evidence for its use in the treatment of cancer. Such as *Scutellariae Radix* (SR), whose dried root is a traditional Chinese medicinal material, which has the functions of clearing heat and drying dampness, purging fire, and detoxifying [4]. The ingredients of SR, baicalin, baicalein, and wogonin, all showed significant inhibitory effects on cancer. Baicalin obviously lowered the viability of OC and bladder cancer cells and inhibited the growth of tumors in mice [5, 6]. And baicalin can induce the ferroptosis of bladder cancer cells by down-regulating FTH1 [7], and of osteosarcoma cells by the Nrf2/xCT/GPX4 axis [8]. Baicalein reduces the ability of OC cells to invade through downregulation of MMP-2 expression [9], and is able to cause apoptosis in lung cancer cells by inhibiting glutamine/m-TOR pathway [10]. Wogonin inhibited the proliferation of several OC cells in a dose- and time-dependent manner, and increased their sensitivity to cisplatin in the study by Feng et al. [11]. The total flavonoid aglycone extracted from SR by Liu et al. showed antitumor activity in pancreatic cancer, inducing apoptosis and autophagy through the PI3 K/Akt/mTOR pathway and inhibiting tumor growth [12].

All these pieces of evidence suggest that SR is a promising anti-cancer herb. Based on the method of network pharmacology, 5,7,2′,6′-Tetrahydroxyflavone (TF) was screened as a key active ingredient of SR, and beta-actin (ACTB) and heat shock protein 90 alpha family class A member 1 (HSP90AA1) were identified to be the key targets of SR. Here, we explored the roles of ACTB and HSP90AA1 in OC, and the effect of TF on OC progression and its mechanism of action through related experiments.

## 2 Materials and methods

### 2.1 Databases

The TCMSP database (https://old.tcmsp-e.com/index.php) was used to screen the active ingredients of SR by setting the screening conditions of oral bioavailability (OB) ≥ 30%, drug-likeness (DL) ≥ 0.18, and Caco-2 permeability (Caco-2) ≥ − 0.4, whose targets were searched using the ETCM database (http://www.tcmip.cn/ETCM/index.php/Home/Index/) and the HERB database (http://herb.ac.cn/). The GeneCards database (https://www.genecards.org/) was used to search the genes related to OC. The protein–protein interaction (PPI) network was constructed using the STRING database (https://cn.string-db.org/) and was visualized by Cytoscape 3.7.1 software. The Weishengxin platform (https://www.bioinformatics.com.cn/login/) was used for making a Venn diagram and performing KEGG analysis. The GSE119056, derived from the Gene Expression Omnibus (GEO) database (https://www.ncbi.nlm.nih.gov/geo/), is a dataset of gene expression in ovarian tumor tissue and normal tissue. The starBase database (https://rnasysu.com/encori/index.php) was used to predict upstream miRNAs of genes.

### 2.2 Cell culture and treatment

OC cell lines (TOV-21G and SK-OV-3) derived from ATCC (America) was cultured using RPMI 1640 medium containing 10% FBS and 1% penicillin/streptomycin. Human ovarian epithelial cells (hOECs) were purchased from Procell (China) and cultured using the hOECs complete culture medium (CM-H055) from the same company. The cell lines listed above have been grown at 37 ℃ with 5% $CO_2$.

TF from MedChemexpress (America) was dissolved into a 10 mM solution with DMSO and stored at − 80 ℃. During the experiment, it was diluted to the corresponding concentration. OC cells were treated with 5, 10, 20, 40, and

60 μM TF for 24 h to explore the effects of different concentrations of TF on their functions. OC cells were treated with 20 μM TF for 24 h for the mechanism exploration. The corresponding volume of DMSO was added as a control (DMSO was diluted at least 166 times).

### 2.3 Cell viability assay

Cell viability was assessed using Cell Counting Kit-8 (CCK-8) from DOJINDO (Japan). First, cells were infected into a 96-well plate with a density of 3000 cells/well. After they were treated by different concentrations of TF for 24 h, the medium containing drug was removed, and then 100 μL of normal medium containing 10% CCK-8 regent was added to each well for 2-h incubation at 37 ℃. Lastly, the optical density (OD) value at 450 nm absorbance was detected by a microplate reader to calculate cell viability: cell viability = [(experimental group OD—blank group OD)/(control group OD—blank group OD)] × 100%.

### 2.4 Transwell migration assay

Cell migration was assessed using transwell inserts (pore size 8 μm, Corning, America). When the OC cells was treated with TF or transfection, they were digested with pancreatic enzymes and centrifuged. The cell precipitation was resuspended in a medium free of FBS, and then 100 μL of cell suspension (about $4 \times 10^4$ cells) was added to the upper chamber. The lower chamber was filled by 500 μL of complete medium containing FBS. After 24 h, the cells in the upper layer of the membrane were erased and the cells in the lower layer were fixed with 4% paraformaldehyde for 15 min and then stained with crystal violet for 20 min. And finally, the positively stained cells were counted under a microscope.

### 2.5 Detection of apoptosis

Apoptotic cells were detected using an Annexin-V- FITC kit (BD Bioscience, America). The OC cells with TF treatment or exogenous transfection were collected after trypsinization and centrifugation. A binding buffer was added to resuspend the cells to be a suspension with a density of $1 \times 10^6$ cells/mL. The cell suspension (100 μL) was mixed with 5 μL of Annexin-V-FITC and 5 μL of PI in an EP tube and incubated at room temperature for 15 min without light. After adding to 400 μL binding buffer, the cells were analyzed using a dual-laser FACS VantageSE flow cytometer (BD Bioscience) to evaluate the percentage of apoptotic cells.

### 2.6 RT-qPCR

Total RNA was extracted from cells using TRIzol reagent (Takara, China). RT-qPCR was performed using the QuantiTect SYBR Green PCR Kit (Sangon Biotech, China). GAPDH and U6 were used for gene normalization. The primer sequences are as follows. Hsa-miR-495-3p: 5′-CGCGTTTGTTTGTACCACGT-3′ (F) and 5′-AGTGCAGGGTCCGAGGTATT-3′ (R); ACTB: 5′-AGATGTGGATCAGCAAGCAGG-3′ (F) and 5′-TGCGCAAGTTAGGTTTTGTCA-3′ (R); HSP90AA1: 5′-GAAGATGACCCTACTGCTGATGATACCAG-3′ (F) and 5′-CGTTACCCCAATCTGTGAAAATAAACCAAC-3′ (R); GAPDH: 5′-GAAACCAGCCAAGTATGATGA-3′ (F) and 5′-TCACTCCTTGGATGCCATG-3′ (R); U6: 5′-GCTTCGGCAGCACATATACTAAAAT-3′ (F) and 5′-CGCTTCACGAATTTGCGTGTCAT-3′ (R). The relative expression of gene or miRNA was calculated by $2^{-\Delta\Delta Ct}$ method.

### 2.7 Cell transfection

The transfection experiment was performed in a 6-well plate, with a 2 mL system which contains 2.5 μg of ACTB/HSP90AA1 or 100 nM of hsa-miR-495-3p inhibitor/mimics, 6 μL of Lipofectamine 2000 (Beyotime, China), and the remaining volume was supplemented by OPTI-MEM medium (Gibco, America). After leaving the mixture for 15 min, it is added to the cells. After 8 h, the transfection mixture was removed, and a fresh medium was added for the follow-up experiments.

### 2.8 Dual-luciferase assay

TOV-21G cells were transfected with 100 ng of a dual-luciferase reporter vector carrying the wild-type (Wt) or mutant (Mut) ACTB/HSP90AA1 fragment (RiboBio, China). Then, 5 nM of hsa-miR-495-3p mimics (mim-495-3p) or negative control

(NC) (MedChemExpress, America) was co-transfected. At 48 h, the luciferase activity was measured using a dual-luciferase reporter gene assay kit (Promega, America) according to the manufacturer's protocols.

### 2.9 Western blotting

The cells were lysed with RIPA buffer for 30 min on the ice. Then the cell lysate was centrifuged (12,000 rpm for 20 min, 4 ℃) to obtain protein supernatant. After the proteins (50 μg) was separated by 10% SDS-PAGE, they were transferred onto the PVDF membrane, which was being enclosed by 5% skim milk for 2 h firstly, and was then incubated with primary antibodies against ACTB (1:1000), HSP90AA1 (1:1000), and GAPDH (1:2000) at 4 ℃ overnight. The next day, the membrane was incubated with the secondary antibody (1:20000) for 1.5 h at room temperature. Finally, the protein signal was evaluated using a BeyoECL Plus Kit (Beyotime) and quantified by ImageJ software.

### 2.10 Statistical analysis

All statistical analyses were performed using the GraphPad Prism 6.0 software. Students'test was used to compare the data between the two groups, and the one-way ANOVA method was used to compare the data among multiple groups. The data were expressed as the mean ± standard deviation. $p < 0.05$ was set as statistically significant.

## 3 Network pharmacological analysis

### 3.1 Potential targets of SR

There were 34 active ingredients of SR were identified through the TCMSP database (Supplementary Table 1), with screening conditions of OB ≥ 30%, DL ≥ 0.18, and Caco-2 ≥ − 0.4. A total of 175 target genes of these ingredients were retrieved using the ETCM and HERB databases to construct the ingredient-target network diagram in the Cytoscape 3.7.1 software (Fig. 1). The node degree value of each ingredient was calculated by the cytoHubba method. The top 5 active ingredients were TF, dihydrooroxylin A (DDRA), 5,7,4'-trihydroxy-6-methoxyflavanone (574-T-6-Ma), wogonin (WGN), and 5,8,2'-Trihydroxy-7-methoxyflavone (582-T-7-M).

### 3.2 SR targets plentiful genes related to OC

We used the GeneCards database to identify 10,763 genes associated with OC, of which 139 genes were targets of SR (Supplementary Fig. 1). By inputting 139 genes into STRING11.0 and setting the minimum interaction score to " > 0.4", 136 genes were obtained. Then, the PPI network diagram was produced via the Cytoscape 3.7.1 software, and the top 20 genes with node degree were selected by the cytoHubba method (Fig. 2).

### 3.3 KEGG analysis

KEGG analysis of 20 genes displayed that they were enriched in a variety of signaling pathways, including the IL-17 signaling pathway, TNF signaling pathway, C-type lectin receptor signaling pathway, and so on (Fig. 3). The figure only shows the signal pathways with the top 10 pathways with *p*-value, and others were shown in Supplementary Table 2.

These shreds of evidence suggest that SR has the potential to inhibit OC progression through multiple targets and pathways.

### 3.4 Inhibition of TF, an active ingredient of SR, on OC progression

TF is the active ingredient of SR with the highest node degree value (56), so it was selected for the mechanism study of this research.

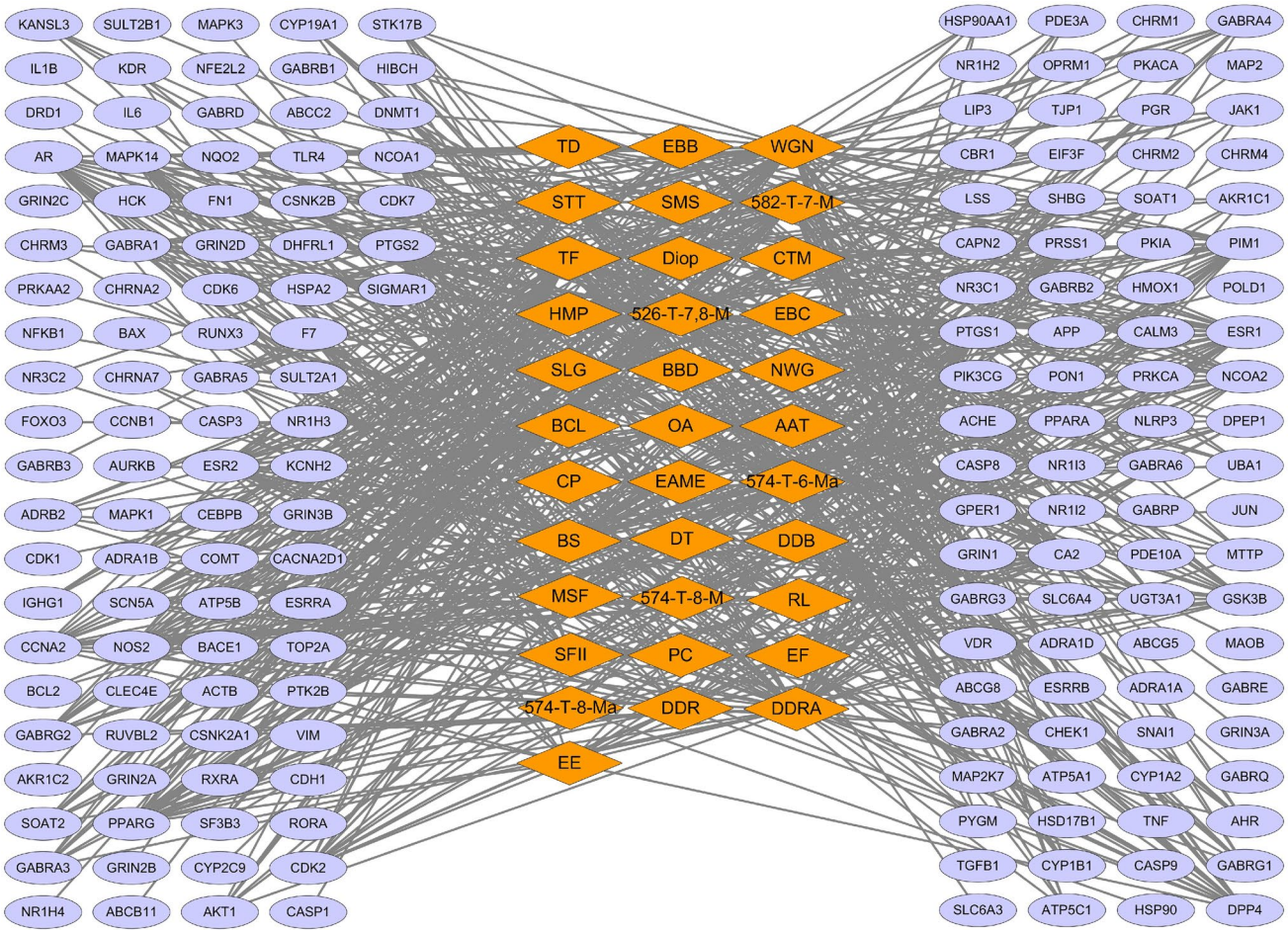


**Fig. 1** The ingredient-target network diagram of SR

### 3.4.1 TF inhibited the functions of OC cells

OC cells were treated with different concentrations of TF for 24 h to detect viability, migration, and apoptosis. The CCK-8 assay displayed that TF concentration-dependently inhibited the viability of OC cells, and inhibited their viability to half at 20 μM (Fig. 4A, B). Therefore, 20 μM of TF was selected for subsequent mechanism experiments. TF also concentration-dependently prevented OC cells from migrating and promoted their apoptosis (Fig. 4C–F). In addition, CCK-8 results showed that 20 μM TF had no significant effect on the viability of hOECs (Supplementary Fig. 2).

### 3.4.2 Regulation of hsa-miR-495-3p on ACTB and HSP90AA1 expression

Among the top 20 OC-related genes with node degree value, 4 genes were the targets of TF, including ACTB, AKT1, ESR1, and HSP90AA1 (Fig. 5A). Since ACTB and HSP90AA1 are rarely studied in OC, we took them as the genes we were interested in. To further explore the mechanism of TF in OC progression, we predicted the upstream miRNAs of ACTB and HSP90AA1 through the starBase database, respectively, and hsa-miR-26b-5p and hsa-miR-495-3p were shared with the miRNAs whose expression were missing in OC tumor tissue (GSE119056) (Fig. 5B). Hsa-miR-495-3p showed higher fold change ($p < 0.01$, log FC = – 3.9) with GEO2R analysis in the GEO database, and it was less studied in cancer, so we chose it as our study object. Supplementary Fig. 3 A and B show the binding sequences of hsa-miR-495-3p to the mRNA of ACTB and HSP90AA1. Hsa-miR-495-3p mimics (mim-495-3p) significantly weakened the luciferase activity in OC cells transfected with the luciferase vector of (wild-type) wt-ACTB or HSP90 AA1, but hardly affected the cells in (mutant) mut-ACTB transfection group (Fig. 5C, D). In addition, hsa-miR-495-3p mimics significantly inhibited the expression of ACTB and HSP90AA1 (Fig. 5E, F).

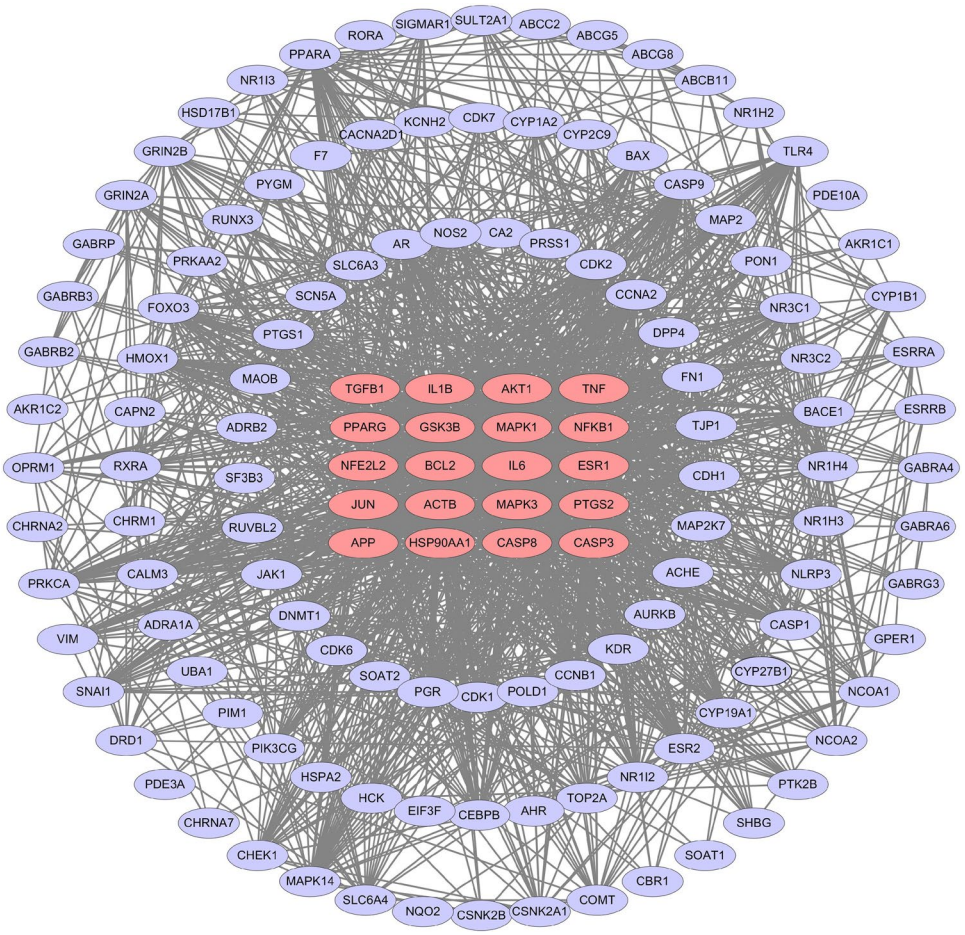


**Fig. 2** The PPT network diagram of SR targets associated with OC

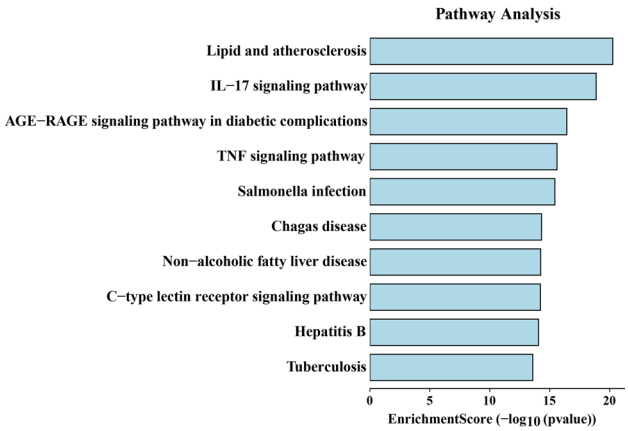


**Fig. 3** KEGG analysis of genes

### 3.4.3 TF regulated the expression of hsa-miR-495-3p/ACTB/HSP90AA1

As shown in Fig. 6A–C and G–I, hsa-miR-495-3p expressed low in OC cells, while ACTB and HSP90AA1 expressed ascendingly. TF significantly upregulated the level of hsa-miR-495-3p (Fig. 6D) and inhibited the expression of ACTB and HSP90AA1 in OC cells, including mRNA (Fig. 6E, F) and protein level (Fig. 6G–I).

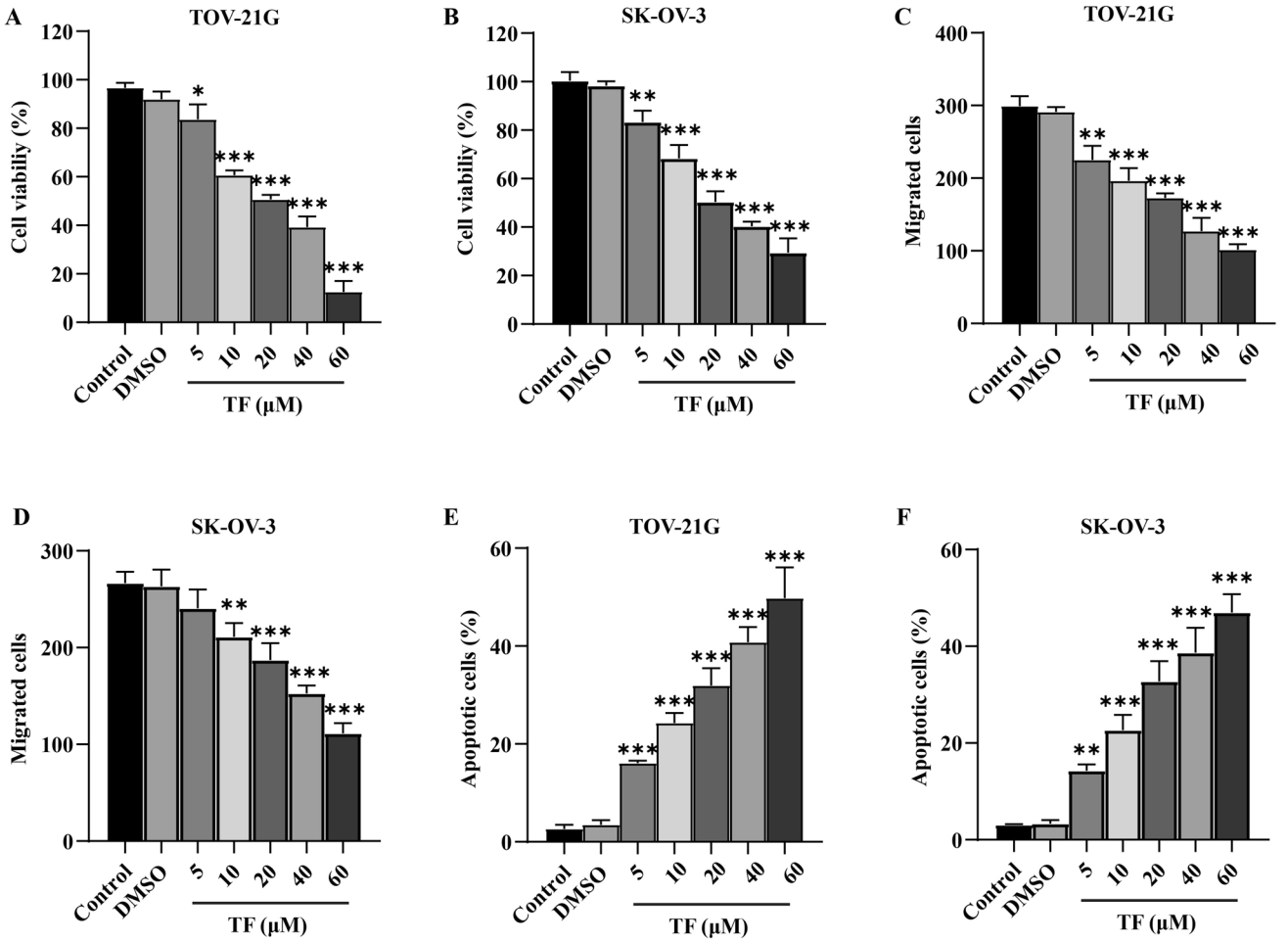


**Fig. 4** Effects of TF on OC cell functions. Effect of TF on OC cell viability (**A**, **B**), migration (**C**, **D**), and apoptosis (**E**, **F**). *$p < 0.05$; **$p < 0.01$; ***$p < 0.001$

### 3.4.4 TF exerted anti-cancer effect through the hsa-miR-495-3p-ACTB/HSP90AA1 pathway

Inhibitor of hsa-miR-495-3p and overexpression of ACTB or HSP90AA1 reversed the decrease of OC cell migration induced by TF (Fig. 7A). In addition, TF up-regulated E-cadherin and down-regulated Vimentin, which was reversed by the hsa-miR-495-3p inhibitor and ACTB or HSP90AA1 overexpression (Fig. 7B, C). Moreover, Up-regulation of hsa-miR-495-3p enhanced the promotion of TF on E-cadherin and Vimentin expression, which was reversed by co-transfection of ACTB/HSP90AA1 overexpressed plasmid (Fig. 7D–F). These findings suggest that TF impeded the epithelial-mesenchymal transition (EMT) process through hsa-miR-495-3p-ACTB/HSP90AA1 pathway, thereby preventing OC cells from migrating.

In addition, down-regulating hsa-miR-495-3p or overexpressing ACTB/HSP90AA1 reversed the increase of apoptosis rate induced by TF (Fig. 7G). RT-qPCR assay showed that TF promoted γ-H2AX and inhibited RAD51 expression, which were reversed by inhibition of hsa-miR-495-3p and overexpression of ACTB or HSP90AA1 (Fig. 7H, I). Western blotting displayed that up-regulation of hsa-miR-495-3p collaborated with TF to promote γ-H2AX and suppressed RAD51 expression, and these effects of hsa-miR-495-3p were weakened by ACTB/HSP90AA1 overexpression (Fig. 7J–L). These results indicate that TF promoted the DNA damage response (DDR) of OC cells through hsa-miR-495-3p-ACTB/HSP90AA1 pathway, thereby leading to the increase of apoptosis rate.

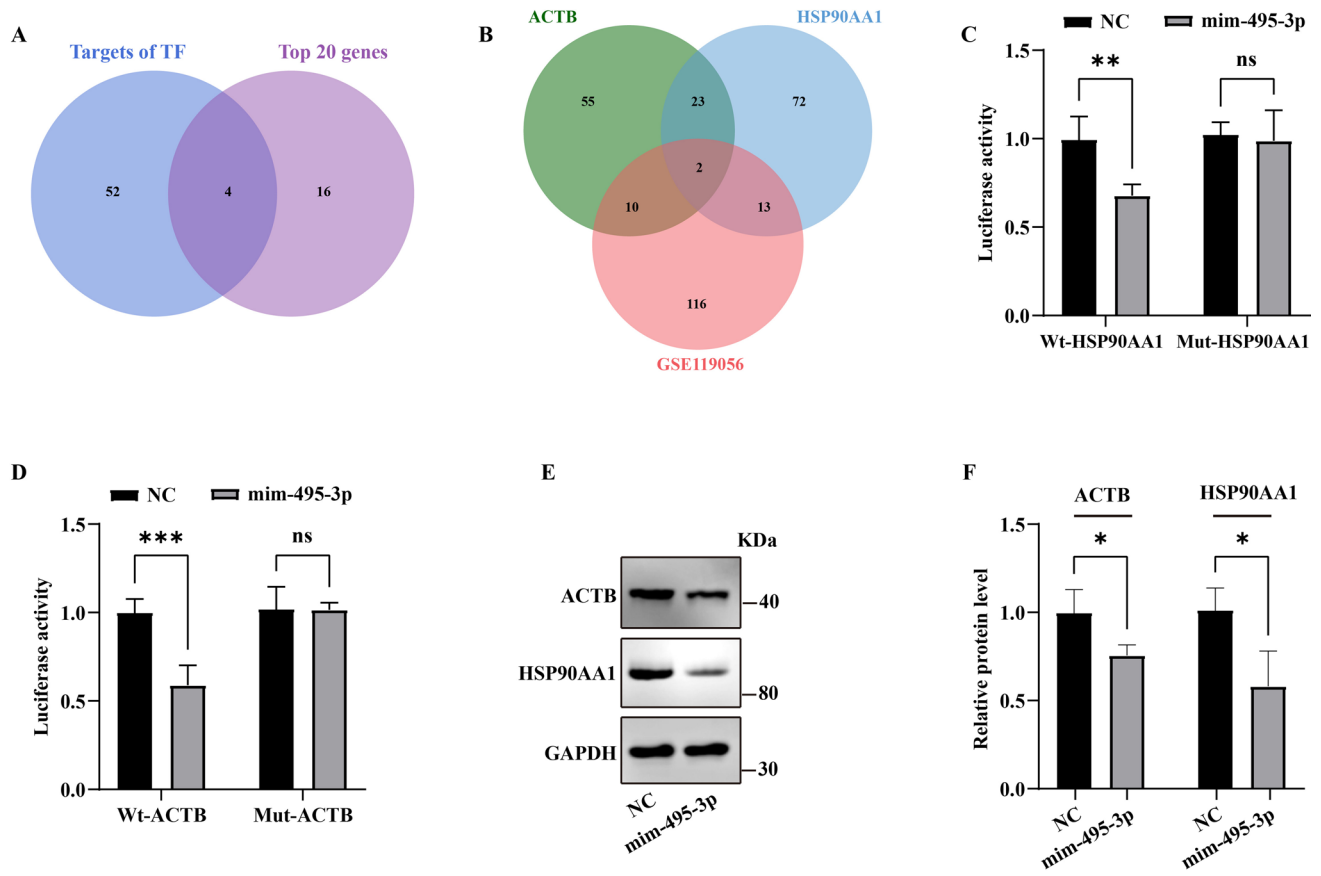


**Fig. 5** Regulation of hsa-miR-495-3p on ACTB and HSP90AA1 expression. The Venn diagram between TF targets and the top 20 genes with node degree value (**A**), and among low-expressed miRNAs in OC tissue (GSE119056) and the upstream miRNAs of ACTB/HSP90AA1 (**B**). **C**, **D** Effects of hsa-miR-495-3p mimics on the luciferase activity in cells transfected with vector of Wt- or Mut-ACTB/HSP90AA1. **E**, **F** Effects of hsa-miR-495-3p mimics on the expression of ACTB and HSP90AA1. *$p < 0.05$; **$p < 0.01$; ***$p < 0.001$; ns, no significant difference

## 4 Discussion

Network pharmacology is a new subject that selects specific signal nodes to design multi-targets of drugs through network analysis of biological systems [13]. This method that was usually used to predict the efficacy and the latent mechanism of drugs by constructing the network of drug-target-disease, and can efficiently screen out the key targets and pathways of drug action on a disease. In this study, using the network pharmacology method, TF, a flavonoid, was identified to be a key ingredient of SR in inhibiting OC progression. ACTB and HSP90AA1 were screened as the key targets of SR to interfere with OC progression. As we described in the introduction, many studies have shown that flavonoids derived from SR, including baicalein, wogonin, etc., which have extensive anti-tumor activities [5, 6, 9–11, 14]. We demonstrated that TF inhibited OC cell viability in a concentration-dependent manner and it restrained EMT-mediated migration and promoted DDR-induced apoptosis through the hsa-miR-495-3p-ACTB/HSP90AA1 pathway in OC cells.

ACTB is a highly conserved cytoskeleton protein widely distributed in eukaryotic cells and plays an important role in cell division and migration [15]. ACTB has been reported to be involved in the development of diversified cancers. ACTB is de-regulated and high-expressed in multiple cancers, such as liver cancer (LC), colorectal cancer (CRC), breast cancer (BC), OC, and so on [16–19]. LC cells with high ACTB expression showed greater aggressiveness [20]. The transduction of MDA7, a tumor suppressor, can significantly decrease the level of ACTB protein, and destroy the cytoskeletal structure to induce the apoptosis of CRC cells [21]. ACTB mediates BC resistance [22]. Salicylic acid can down-regulate ACTB to induce apoptosis of BC cells by [23]. In general, although the abnormal expression of ACTB in cancer has been widely confirmed, the molecular mechanisms involved have rarely been explored.

HSP90AA1 is a molecular chaperone that regulates target proteins involved in cell cycle and signal transduction. HSP90 AA1 promotes lymphatic metastasis of hypopharyngeal squamous cell carcinoma by inducing EMT [24].

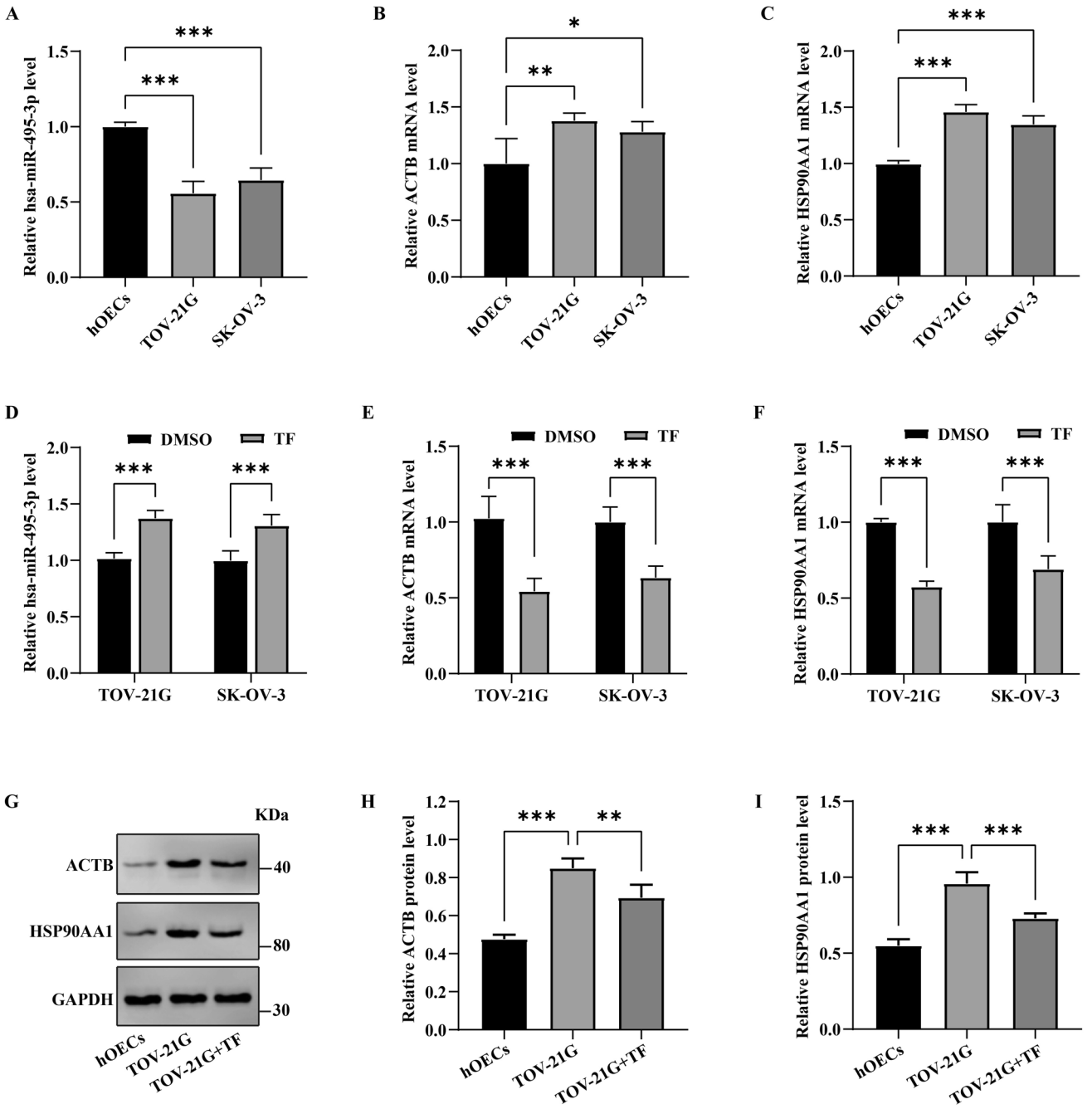


**Fig. 6** TF regulated the expression of hsa-miR-495-3p/ACTB/HSP90AA1. **A**–**C** The expression of hsa-miR-495-3p, ACTB, and HSP90AA1 in hOECs and OC cells. **D**–**F** Effects of TF on hsa-miR-495-3p, ACTB, and HSP90AA1 expression. **G**–**I** Effect of TF on the protein expression of ACTB and HSP90AA1

Upregulation of HSP90AA1 is associated with lower overall survival in BC patients [25]. In CRC, DAB2IP can downregulate HSP90AA1 to restrain the malignant phenotypes of tumor cells [26]. HSP90AA1 has been shown that increase chemotherapy resistance of osteosarcoma cells by inducing autophagy and inhibiting apoptosis [27]. Apigenin can hinder the development of colon cancer (CC) by targeting HSP90 AA1 [28]. There is only one report on the function of HSP90AA1 in OC: HSP90AA1 has been certificated to aid OC cell survival, and its high level can increase OC cell resistance to cisplatin [29].

MiRNAs are a class of short non-coding RNAs that are widely involved in human diseases. The anti-cancer effect of hsa-miR-495-3p has been reported in many studies. Hsa-miR-495-3p can prevent CC cells from growing and migrating by

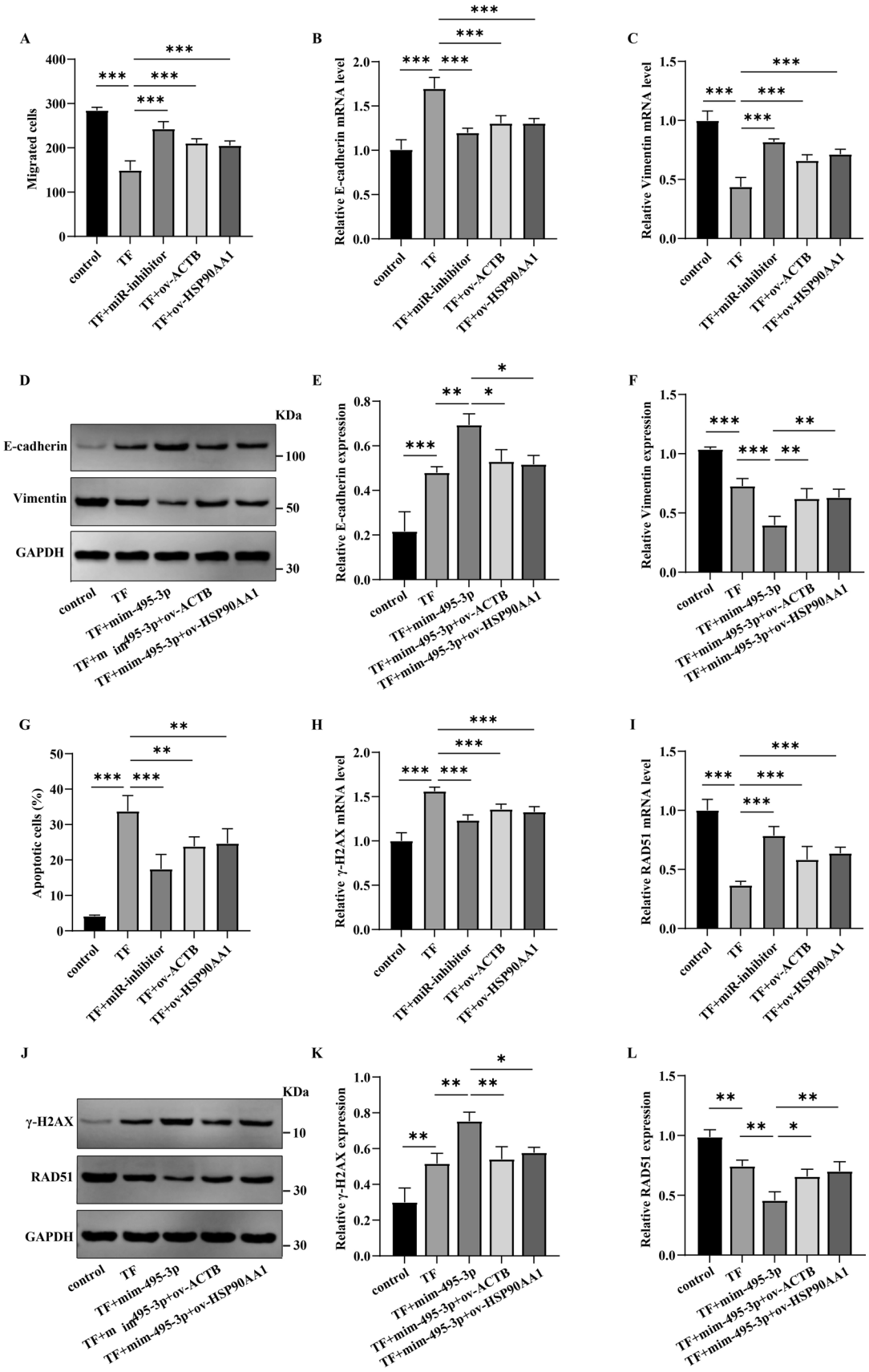


**Fig. 7** Mechanism of TF inhibiting OC cell functions. Effects of hsa-miR-495-3p, ACTB and HSP90AA1 on migration (**A**) and apoptosis (**G**) and the expression of E-cadherin/Vimentin (**B**–**F**) and γ-H2 AX/RAD51 (**H**–**L**) in TF-treated OC cells. *$p < 0.05$; **$p < 0.01$; ***$p < 0.001$;

inhibiting HMGB1 [30]. Hsa-miR-495-3p targeted CDK1 together with hsa-miR-143-3p, thereby inhibiting the progression of cervical cancer [31]. LncRNA FAM83 A-AS1 aggravates the malignant progression of esophageal cancer by reducing the hsa-miR-495-3p level [32]. LINC01133 reduces its cellular level by adsorption of miR-495-3p, thereby promoting TPD52 expression, which contributes to the transfer of epithelial OC [33].

The process by which cells lose their epithelial properties and gain the interstitial properties is called EMT, which contributes to the metastasis of cancer cells [34]. Deletion of E-cadherin expression and abnormal expression of Vimentin are markers of EMT and are relevant to an enhancive risk of cancer metastasis [35]. Cancer cells can resist death and drug treatment by escaping DDR, accompanied by inhibition of DDR-associated proteins (such as γ-H2AX) and abnormal expression of DDR repair proteins (such as RAD51) [36]. The results of this study displayed that TF significantly up-regulated E-cadherin and γ-H2AX, and down-regulated Vimentin and RAD51 in OC cells, which were reversed by inhibition of hsa-miR-495-3p and overexpression of ACTB or HSP90AA1, suggesting that TF could inhibit the migration and promote the apoptosis of OC cells by the hsa-miR-495-3p-ACTB/HSP90AA1 pathway-mediated EMT and DDR.

In summary, we have identified a new flavonoid derived from SR, that is TF. TF effectively inhibited the functions of OC cells through the hsa-miR-495-3p-ACTB/HSP90AA1 pathway. Our study will provide a valuable theoretical basis for the application of SR in OC treatment.

**Acknowledgements** Not applicable.

**Author contributions** Conceptualization, M.C., H.J. and Z.S.; Data curation, M.C. and H.J.; Formal analysis, X.T. and Y.J.; Funding acquisition, M.C. H.J. and Z.S.; Investigation, X.T. and Y.J.; Methodology, M.C. and H.J.; Project administration, Z.S.; Resources, X.T. and Y.J.; Software, X.T. and Y.J.; Supervision, Z.S.; Validation, X.T. and Y.J.; Visualization, M.C. and H.J.; Roles/Writing—original draft, M.C. and H.J.; Writing—review & editing, Z.S.

**Funding** The authors declare that no funds, grants, or other support were received during the preparation of this manuscript.

**Data availability** The datasets used and/or analysed during the current study are available from the corresponding author on reasonable request.

## Declarations

**Ethics approval** Not applicable.

**Consent to participate** Informed consent was obtained from all individual participants included in the study.

**Consent for publication** Not applicable.

**Competing interests** The authors declare no competing interests.



## References

1. Zhang R, Siu MKY, Ngan HYS, Chan KKL. molecular biomarkers for the early detection of ovarian cancer. Int J Mol Sci. 2022. https://doi.org/10.3390/ijms231912041.
2. Moufarrij S, Dandapani M, Arthofer E, Gomez S, Srivastava A, Lopez-Acevedo M, et al. Epigenetic therapy for ovarian cancer: promise and progress. Clin Epigenet. 2019;11(1):7.
3. Arnaoutoglou C, Dampala K, Anthoulakis C, Papanikolaou EG, Tentas I, Dragoutsos G, et al. Epithelial ovarian cancer: a five year review. Medicina. 2023. https://doi.org/10.3390/medicina59071183.
4. Banik K, Khatoon E, Harsha C, Rana V, Parama D, Thakur KK, et al. Wogonin and its analogs for the prevention and treatment of cancer: a systematic review. Phytother Res. 2022;36(5):1854–83.
5. Ikemoto S, Sugimura K, Yoshida N, Yasumoto R, Wada S, Yamamoto K, et al. Antitumor effects of Scutellariae radix and its components baicalein, baicalin, and wogonin on bladder cancer cell lines. Urology. 2000;55(6):951–5.
6. Gao C, Zhou Y, Li H, Cong X, Jiang Z, Wang X, et al. Antitumor effects of baicalin on ovarian cancer cells through induction of cell apoptosis and inhibition of cell migration in vitro. Mol Med Rep. 2017;16(6):8729–34.

7. Kong N, Chen X, Feng J, Duan T, Liu S, Sun X, et al. Baicalin induces ferroptosis in bladder cancer cells by downregulating FTH1. Acta Pharm Sin B. 2021;11(12):4045–54.
8. Wen RJ, Dong X, Zhuang HW, Pang FX, Ding SC, Li N, et al. Baicalin induces ferroptosis in osteosarcomas through a novel Nrf2/xCT/GPX4 regulatory axis. Phytomedicine. 2023. https://doi.org/10.1016/j.phymed.2023.154881.
9. Yan H, Xin S, Wang H, Ma J, Zhang H, Wei H. Baicalein inhibits MMP-2 expression in human ovarian cancer cells by suppressing the p38 MAPK-dependent NF-kappaB signaling pathway. Anticancer Drugs. 2015;26(6):649–56.
10. Li J, Zhang D, Wang S, Yu P, Sun J, Zhang Y, et al. Baicalein induces apoptosis by inhibiting the glutamine-mTOR metabolic pathway in lung cancer. J Adv Res. 2024. https://doi.org/10.1016/j.jare.2024.02.023.
11. Xing F, Sun C, Luo N, He Y, Chen M, Ding S, et al. Wogonin increases cisplatin sensitivity in ovarian cancer cells through inhibition of the phosphatidylinositol 3-kinase (PI3K)/Akt pathway. Med Sci Monit. 2019. https://doi.org/10.1265/MSM.913829.
12. Liu J, Wang H, Wang J, Chang Q, Hu Z, Shen X, et al. Total flavonoid aglycones extract in Radix Scutellariae induces cross-regulation between autophagy and apoptosis in pancreatic cancer cells. J Ethnopharmacol. 2019. https://doi.org/10.1016/j.jep.2019.02.005.
13. Nogales C, Mamdouh ZM, List M, Kiel C, Casas AI, Schmidt H. Network pharmacology: curing causal mechanisms instead of treating symptoms. Trends Pharmacol Sci. 2022;43(2):136–50.
14. Gu Y, Zheng Q, Fan G, Liu R. Advances in anti-cancer activities of flavonoids in scutellariae radix: perspectives on mechanism. Int J Mol Sci. 2022. https://doi.org/10.3390/ijms231911042.
15. Bunnell TM, Burbach BJ, Shimizu Y, Ervasti JM. beta-actin specifically controls cell growth, migration, and the G-actin pool. Mol Biol Cell. 2011;22(21):4047–58.
16. Kwon MJ, Oh E, Lee S, Roh MR, Kim SE, Lee Y, et al. Identification of novel reference genes using multiplatform expression data and their validation for quantitative gene expression analysis. PLoS ONE. 2009;4(7):e6162.
17. Li YL, Ye F, Hu Y, Lu WG, Xie X. Identification of suitable reference genes for gene expression studies of human serous ovarian cancer by real-time polymerase chain reaction. Anal Biochem. 2009;394(1):110–6.
18. Morse DL, Carroll D, Weberg L, Borgstrom MC, Ranger-Moore J, Gillies RJ. Determining suitable internal standards for mRNA quantification of increasing cancer progression in human breast cells by real-time reverse transcriptase polymerase chain reaction. Anal Biochem. 2005;342(1):69–77.
19. Waxman S, Wurmbach E. De-regulation of common housekeeping genes in hepatocellular carcinoma. BMC Genomics. 2007. https://doi.org/10.1186/1471-2164-8-243.
20. Gao Q, Wang XY, Fan J, Qiu SJ, Zhou J, Shi YH, et al. Selection of reference genes for real-time PCR in human hepatocellular carcinoma tissues. J Cancer Res Clin Oncol. 2008;134(9):979–86.
21. Blanquicett C, Johnson MR, Heslin M, Diasio RB. Housekeeping gene variability in normal and carcinomatous colorectal and liver tissues: applications in pharmacogenomic gene expression studies. Anal Biochem. 2002;303(2):209–14.
22. Khimani AH, Mhashilkar AM, Mikulskis A, O'Malley M, Liao J, Golenko EE, et al. Housekeeping genes in cancer: normalization of array data. Biotechniques. 2005;38(5):739–45.
23. Ferreira E, Cronje MJ. Selection of suitable reference genes for quantitative real-time PCR in apoptosis-induced MCF-7 breast cancer cells. Mol Biotechnol. 2012;50(2):121–8.
24. Tang F, Li Y, Pan M, Wang Z, Lu T, Liu C, et al. HSP90AA1 promotes lymphatic metastasis of hypopharyngeal squamous cell carcinoma by regulating epithelial-mesenchymal transition. Oncol Res. 2023;31(5):787–803.
25. Liu H, Zhang Z, Huang Y, Wei W, Ning S, Li J, et al. Plasma HSP90AA1 predicts the risk of breast cancer onset and distant metastasis. Front Cell Dev Biol. 2021. https://doi.org/10.3389/fcell.2021.639596.
26. Zhang M, Peng Y, Yang Z, Zhang H, Xu C, Liu L, et al. DAB2IP down-regulates HSP90AA1 to inhibit the malignant biological behaviors of colorectal cancer. BMC Cancer. 2022;22(1):561.
27. Xiao X, Wang W, Li Y, Yang D, Li X, Shen C, et al. HSP90AA1-mediated autophagy promotes drug resistance in osteosarcoma. J Exp Clin Cancer Res. 2018;37(1):201.
28. Sain A, Khamrai D, Kandasamy T, Naskar D. Apigenin exerts anti-cancer effects in colon cancer by targeting HSP90AA1. J Biomol Struct Dyn. 2023. https://doi.org/10.1080/07391102.2023.2299305.
29. Chu SH, Liu YW, Zhang L, Liu B, Li L, Shi JZ, et al. Regulation of survival and chemoresistance by HSP90AA1 in ovarian cancer SKOV3 cells. Mol Biol Rep. 2013;40(1):1–6.
30. Zhang JL, Zheng HF, Li K, Zhu YP. miR-495–3p depresses cell proliferation and migration by downregulating HMGB1 in colorectal cancer. World J Surg Oncol. 2022;20(1):101.
31. Tang J, Pan H, Wang W, Qi C, Gu C, Shang A, et al. MiR-495-3p and miR-143-3p co-target CDK1 to inhibit the development of cervical cancer. Clin Transl Oncol. 2021;23(11):2323–34.
32. Huang GM, Zang HL, Geng YX, Li YH. LncRNA FAM83A-AS1 aggravates the malignant development of esophageal cancer by binding to miR-495–3p. Eur Rev Med Pharmacol Sci. 2020;24(18):9408–15.
33. Liu S, Xi X. LINC01133 contribute to epithelial ovarian cancer metastasis by regulating miR-495-3p/TPD52 axis. Biochem Biophys Res Commun. 2020;533(4):1088–94.
34. Zhang N, Ng AS, Cai S, Li Q, Yang L, Kerr D. Novel therapeutic strategies: targeting epithelial-mesenchymal transition in colorectal cancer. Lancet Oncol. 2021;22(8):e358–68.
35. Luo T, Wang L, Wu P, Gong W, Chen W, Zhao H, et al. Downregulated vimentin and upregulated E-cadherin in T1 stage non-small-cell lung cancer: does it suggest a mesenchymal-epithelial transition? Neoplasma. 2017;64(5):693–9.
36. Thielhelm TP, Goncalves S, Welford S, Mellon EA, Bracho O, Estivill M, et al. Primary vestibular schwannoma cells activate p21 and RAD51-associated DNA repair following radiation-induced DNA damage. Otol Neurotol. 2021;42(10):e1600–8.